REALTIME MONITORING INSTRUMENT RELIABILITY OF THREE PHASE INDUCTION MOTOR BEARING BASED ON NEURAL NETWORK (NN) ANALYSIS

[1] **BAMBANG SRI KALOKO**, [2] **MALIKUL FANANI**,

[1] Department of Electrical Engineering, Faculty of Engineering, University of Jember, Sumbersari, Jember, Indonesia

[2] Department of Electrical Engineering Student, Faculty of Engineering, University of Jember, Sumbersari, Jember, Indonesia

E-mail: bambangsrikaloko@yahoo.com; kaloko@unej.ac.id[1]

ABSTRACT

Three-phase induction motors are one of the most widely used drives in industry and transportation because of their simple construction and reliability. Damage to the induction motor affects the existing production process. Therefore, early detection of induction motor damage is needed to avoid further damage and cause losses to the industry. The method of identifying bearing damage to the induction motor uses a no-load condition. The combination of FFT transformation and artificial neural net is used as a method of identifying the damage. The identification variable used in the method is taken from the stator current signal. To achieve the desired goal, the experimental data used are 10%, SEF 24%. bearing damage to the inside, the outside ball, and the separator. Simulation results show that protoype is able to read 85% of the identified training data for each type of damage

Keywords: *Early Detection, Bearing Damage, Artificial Neural Network, Induction Motor*

1. INTRODUCTION

Induction motor is one of the driving motors that are often used in the industrial world as the main driver in the production process activities. The use of induction motors is mainly for milling machines, elevators, conveyors, screw conveyors, and various other movers. The use of an induction motor as a propeller in addition to having advantages also has problems, one of which is mechanical and electrical stress.

Bearing damage is the most common damage in industrial motor problems, reaching 152, then 75 for winding and 2 rotor damage [1]. Whereas electrical stress is caused by high frequencies of current generated in the rotor, high overvoltage is caused by AC drive reflections from transient voltage waves. This electrical stress can cause short circuit winding which means the total damage to the induction motor [2].

If induction motor damage that occurs is not detected in the initial stages, then it will result in severe damage with various types of damage that occurs. Damage to the motor that is not detected will result in a shutdown or cessation of the production process that is long enough, the cost of repairing motor components that must be charged, and loss of raw materials that must be processed will be hampered due to motor damage, resulting in disruption of the company's production process.

At present, there are several ways to monitor motor damage by using vibration monitoring, temperature monitoring, chemical properties monitoring and monitoring acoustic emissions, but all of these monitoring requires expensive sensors or special tools. However, it is different from monitoring that uses current because it does not require additional sensors. This is what causes the current monitoring to be associated with the basic amount of electricity in the electromechanical design which includes the current and voltage for making measurements. The results of the use of current monitoring are non-intrusive and can even be implemented at the motor control center remotely.

Based on the background and problems above, one of the methods used to detect damage to induction motors that often occur in motor bearings is to use the method of detecting the type of damage and the level of damage concerning the characteristics of the current signal using Neural network analysis. This method is one that is suitable to be applied as an economical machine conditioning monitoring, namely maintenance and preventive

management based on monitoring the condition of the engine.

In subsequent studies, the detection tool of induction motor bearing reliability only uses the fast Fourier transform method. In this study, it will be continued by adding the FFT graph output to be processed using the Neural Network method. The use of neural networks is intended so that the detection carried out by reading the prototype can be maximized again. The data needed to train the Neural network is generated in the Electric Energy Conversion Laboratory using a three-phase induction motor specifically designed to facilitate the simulation of detection of motor damage that indicates damage to the bearing.

2. LITERATURE REVIEW

2.1 Induction Motor

Three-phase induction motor is the most common motor used in the motor drive in industries. The three-phase motor contains two main components that are stator and rotor. Work principal from induction motor is based on the rotating field that is stator containing three windings electrically in the angle of 120^0 exist as Figure 2.5 below.
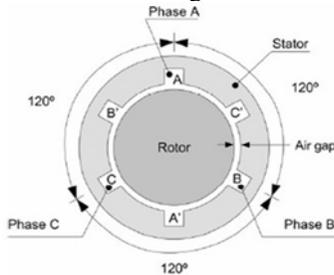

Figure 1. Induction Motor Schematic

When connecting three-phase sources on the induction motor terminal, it will cause the existing sinusoidal alternating current of I_R, I_S, I_T flowing to the stator.
Electrical energy will be supplied to the induction motor by 3 phase system that has a phase of 120^0 (2Ꙥ/3 Radian).

$$Va = Vm \cos (\omega t) \qquad (1)$$

$$Vb = Vm \cos \left(\omega t - \frac{2\pi}{3}\right) \qquad (2)$$

$$Vc = Vm \cos \left(\omega t + \frac{2\pi}{3}\right) \qquad (3)$$

In this case, Va is the current on phase of A and Vb is the current flowing to phase of B and Vc is the current flowing to phase of C, Vm is the peak value from fundamental frequency from each phase, and ω is the angular velocity (rad/s) because of the

symmetric phase difference, the total amount of three phases is zero.

$$Ia + Ib + Ic = 0 \qquad (4)$$

With the value of the current angle on the phase difference of 120^0

$$Ia = Im \cos (\omega t - \varphi) \qquad (5)$$

$$Ib = Im \cos \left(\omega t - \varphi - \frac{2\pi}{3}\right) \qquad (6)$$

$$Ic = Im \cos (\omega t - \varphi + \frac{2\pi}{3}) \qquad (7)$$

I_a is the phase current of A and I_b is phase of B and I_c is phase of C, and I_m is the peak value of fundamental frequency from each phase, ω is the angular velocity (rad/s). φ is power factor of lagging and t is time (s) caused by the phase shifting with the angle length of 120^0, the total amount of three phases is zero.

$$Ia + Ib + Ic = 0 \qquad (8)$$

2.2 Speed of Synchronous. Asynchronous, and Slip

Speed filter of rotating field in the induction motor is called synchronous speed. The value of induction motor synchronous speed with p pole in rpm is:

$$n_{syn} = \frac{120f}{p} \qquad (9)$$

f is the value of stator frequency (Hz), n_{syn} is the value of synchronous speed because rotor rotates on the asynchronous speed usually slow from the synchronous speed toward fast speed. The difference of this speed value is called slip speed,

$$n_s = n_{syn} - n_{asyn} \qquad (10)$$

Where n_{syn} is the speed on the rotor (rpm) and n_s is slip speed. On the motor slip speed with the unit of s (slip/unit):

$$s = \frac{n_{syn} - n_{syn}}{n_{syn}} \qquad (11)$$

On the motor synchronous speed produced, it depends on the frequency from the source voltage and amount of poles. Asynchronous speed or rotor speed does not only depend on the number of poles and frequency, but load torque on the motor is also having an effect. The higher the load torque, the higher the slip, and the slower rotor speed.

2.3 Types of Induction Motor Damage
2.3.1 Eccentricity

The damage on the eccentricity is defined as the damage occurred on the condition of asymmetric air-gap between stator and rotor. The giving of the standard level is intended to maintain the eccentricity level as low as possible aiming to decrease the vibration and noise and minimize unbalance magnetic pull (UMP) [3]. It aims to air-

gap induction motor very low so that the induction motor is very sensitive on the change of air-gap length [4].

Based on the types of eccentricity there are two types that are static and dynamic eccentricity. Static eccentricity is caused by the minimum position of radial length from the air-gap on the certain distance, while dynamic eccentricity is caused by navel rotor that is not on the center point of rotation and minimum position so that air-gap also rotates together with the rotor. There are examples of eccentricity.
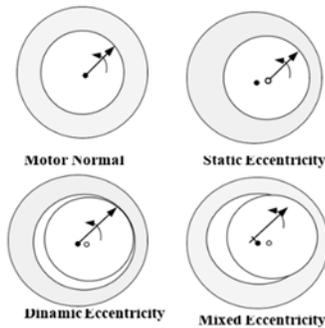

Figure 2. Types of Eccentricity

2.3.2 Inner Raceway Fault

The number of excitation frequency is caused by local fault impulse on the inner raceway in the bearing expressed in the equation as follows:

$$f_i = \frac{N_n}{2} f_r \left(1 + \frac{D_b cos\theta}{D_p} \right) \qquad (13)$$

2.3.3 Outer Raceway Fault

The number of impulse excitation caused on the local fault of outer bearing can be expressed with the equation as follows:

$$f_o = \frac{N_n}{2} f_r \left(1 - \frac{D_b cos\theta}{D_p} \right) \qquad (14)$$

2.3.4 Ball Fault

If there is a fault on the ball, the frequency of Ball Fault can be calculated by the below equation:

$$f_b = \frac{N_n}{2D_b} f_r \left(1 - \left(\frac{D_b cos\theta}{D_p} \right)^2 \right) \qquad (15)$$

2.3.5 Cage

If there is a fault on the cage. The magnitude of cage fault can be seen in the below equation:

$$f_c = \frac{1}{2} f_r \left(1 - \frac{D_b cos\theta}{D_p} \right) \qquad (16)$$

2.4 Jaringan Saraf Tiruan

neural network is an information processing system with certain characteristics that are made to resemble a human biological network. For example n pieces of input and weighers, the output function of each neuron is as follows:

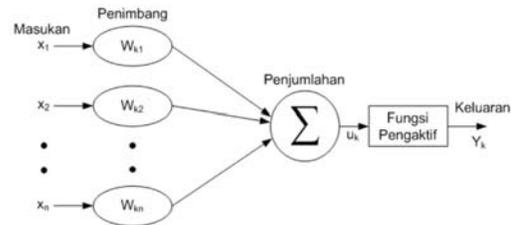$$F(x,w) = f(w_1 x_1 + \cdots + w_n x_n) \qquad (17)$$

Figure 3. Neuraon model without bias

The learning process (learning) for ANN is a process of regulating the value of the weighting weights to get the best value by training ANN to use a set of data, according to the desired system performance [5].

2.5 Backpropogation Neural Network

The BPNN training algorithm consists of two the main process, i.e. feed forward and backpropagation of the error [6]. In a line large, this algorithm is referred to as backpropagation neural network (BPNN) because when ANN is given an input pattern as a pattern training, then the pattern is spread forward (forward) to units in the hidden layer and passed on to the output layer to be provide a response referred to as ANN output. When the output of ANN is not the same with the expected output then the output will be spread backward (backward) on the hidden layer and forwarded to the unit in the input layer.

3. MATERIAL AND METHOD

The motor current reversal sensor uses a current transformer to obtain a signal with a maximum magnitude that is unable to use analog to digital converter (ADC) equipment. Furthermore, this analog signal will move with the ADC into a digital signal. The digital signal will then be processed by Intel Galileo microprocessors by reading an array of 10,000 data, then the results of these results are sent through the Intel Galileo serial port and processed using discrete FFT transformation up to level three. These high-frequency signals are then taken from each feature and then inputted to the acquisition system (ANN). From this system, the signal will be identified whether the motor fixes the fault or not.

The flow diagram of the induction motor bearing damage detection in this research can be seen in Figure 1 below.
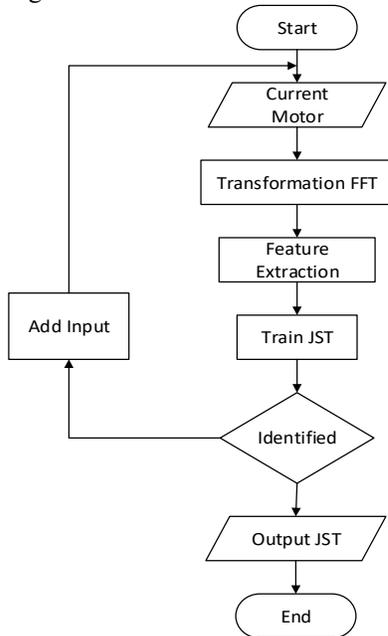

Figure 4. Flow Chart of Induction Motor Bearing Damage Detection

3.1 Test Equipment

In this research, using a 3 phase induction motor. The motor will be arranged according to Figure 7. The induction motor used in 3 phases with a power of 0.37 KW. For induction, motor data-sheet can be seen in Table 1 below.

Tabel 1. Induction Motor Specifications

No	Parameter	Value
1	Power	0,37 kW
2	Frequency (Hz)	50 Hz
3	Volt	220/380 V
4	Current	1,12 A
5	Air-Gab	4 mm
6	Insulation Class	B
7	Speed	1400 Rpm
8	Phase	3
9	Production	Taizhgou Yu Ba Electric Co.,Ltd.
10	Model	YS 712-4

Then the bearings used in this study are ball bearing types with serial number 6203RS. The datasheet can be seen in table 2 below.

Table 2. Bearing Specifications

No	Parameter	Information
1.	Seals	2
2.	Bahan	Standart SAE 52100
3.	Bore	17 mm
4.	Outside Diameter	40 mm
5.	*Width (lebar)*	12 mm
6.	No. Balls	8
7.	Ball Diameter	¼
8.	Static Load	890 lbs
9.	Dynamic Load	150 lbs

Figure 5. Bearing View Upper

In this experiment, bearing damage and eccentricity were divided into 6 types of damage, namely SEF 10% and 24% SEF. bearing damage to the inside, the outside ball, and the separator.

3.2 Test and Train

In this experiment analog data from the motor stator current is converted into digital data using an A / D converter and then displayed through an oscilloscope to determine the waveform to be analyzed. This digital data is sent to a computer via a serial cable (RS-232) with the help of a remote control program which will later be used as input in the learning process on ANN to determine the state of the motor. Analog to digital converter is needed because the motor stator current data is analog data so it needs to be converted into a discrete data form to facilitate the next process. This A / D converter also functions as a converter of current data to voltage data because the oscilloscope input is voltage data. Schematic of the test circuit can be seen in Figure 3 as follows.
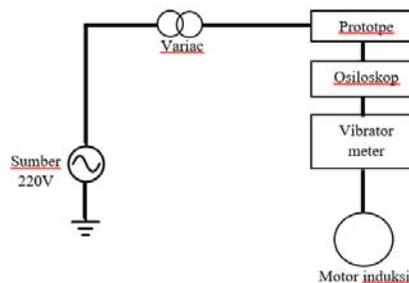

Figure 6. Testing Schematic Diagram

3.3 Data Collection

At the stage of data retrieval, the stator current waveforms of the normal and induction motor are induced. The data collection form of the induction motor stator current is done by installing a prototype on the phase cable on the supply side. This data collection includes SEF 10%, SEF 24%, and bearing damage on the inside, outside, ball section and separator section. The waveform data obtained is then sent to the computer via a serial cable (RS232) using the help of the GRS-60X2 PC remote control program. The files generated by this program are data in CSV format and waveform images in BMP, PCX, TIFF, PNG or JPEG formats. The program display can be seen in Figure 4
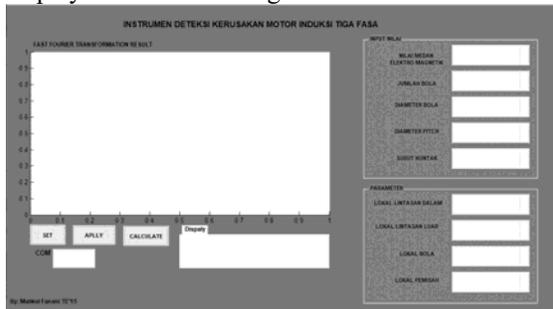

Figure 7. Display Remote Program Control

3.4 Data Processing

In a previous study, the disintegration of feature time alone was carried out. therefore in this study, the data from the FFT wave results obtained from the two data collection processes are grouped into two. The first data is the data that will be used as input in the learning process of ANN. The second data is a test to determine the ANN labor that will be used. Furthermore, each group of data is processed using FFT to get the feature extraction of each wave. This step is an important start in monitoring and detecting motor damage because it can reduce the number of sampling to speed up the calculation process in ANN training. The use of FFT as a data processor because the current signal at the time of the disturbance is a non-stationary or transient signal. So that the situation can be used as a sign of induction motor interference. Because different disturbances have different effects on wavelet transform stator currents can be used as a feature extraction method.

3.5 Identification Stage

For learning purposes, the NN parameters that must be determined are as follows:

1. Learning function: trained (Gradient descent-backpropagation).
2. Number of layers
   - Input layer: 22 neurons
   - Hidden layer: 1500 neurons
   - Output layer: 4 neurons
3. Activation function
   - Hidden layer: tansig (sigmoid bipolar)
   - Output layer: logsin (sigmoid binary)
4. Maximum iteration: 200,000
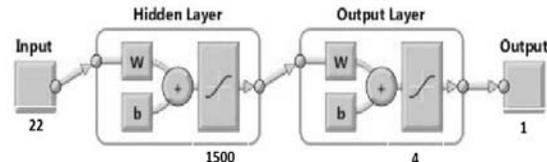5. Minimum error: 10e-5
6. Learning rate: 0.1

Figure 8. Neural Network

ANN output is an identification of the state of the induction motor. The resulting indications include the presence or absence of a short bearing on the reliability of the induction motor. Identification of the state of the induction motor can be seen in Table 3.

Tabel 3. Identification of Induction Motor Conditions

Induction Motor	Output ANN
Normal	[1 0 0 0 0 0]
SEF 10%	[0 1 0 0 0 0]
SEF 24%	[0 0 0 1 1 0]
Inner Race Fault	[0 0 0 0 1 1]
Outer Race Fault	[1 1 1 0 0 0]
Rolling Element	[0 1 1 1 0 0]

3.6 Diagram Block of System

On this research this time in order to obtain the expected data and associated with the first goal from the topic taken, the form of the diagram block of the system, on the whole, can be seen in the below figure:

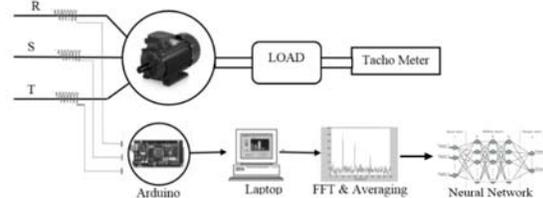*Figure 9. Diagram Block of System*

3.7 Testing Circuit

In this testing of motor-load is connected to transformer variable (variac) that is previously connected to a source of 220 V. Schematic of circuit testing can be seen in the below figure.
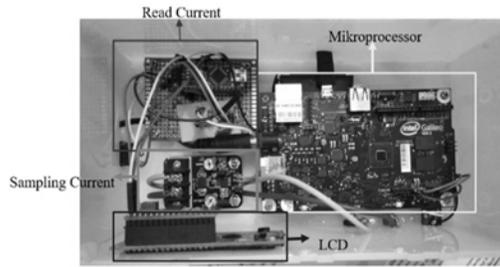
Figure 10. Circuit of Prototype

IV. RESULT AND DISCUSSIONS

From the measurements of the three-phase induction motor which is done so that the waveform is obtained which has been converted into a time-domain through the FFT sampling process. The following is the result of sampling the induction motor current shown in the figure below.
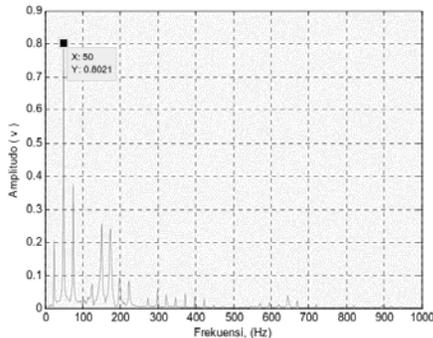
Figure 11. Plot Grafik FFT Normal State
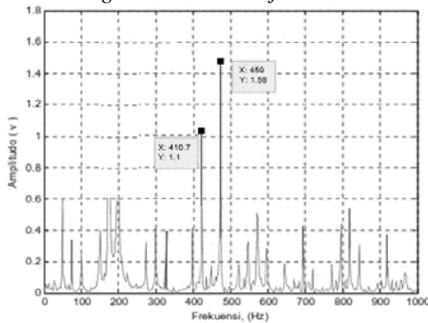
Figure 12. Plot Grafik FFT SEF 10%
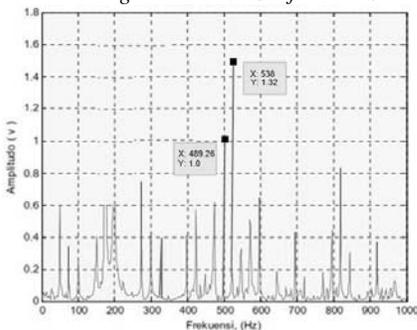
Figure 13. Plot Grafik FFT SEF 24%
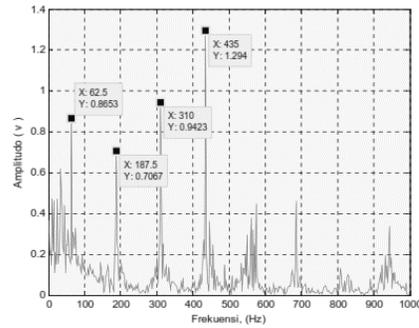
Figure 14. Plot Grafik Inner Race Fault
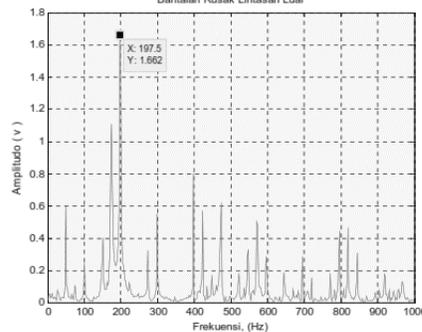
Figure 15. Plot Grafic Outer Race Fault
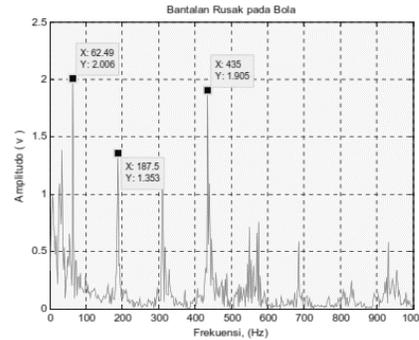
Figure 16 . Plot Grafik Rolling Element

4.1 Feature Extraction

From the results of the decomposition of the current through the things level, high-frequency signal features are obtained which can be used as an indication of damage to the induction motor as shown in tables 4, 5, 6, 7, 8,9,10,11 and 12,13 below.

Table 4. Normal Current Feature

Signal Feature						
Nor mal	me d	ma ks	mi n	Std ev	|Med dev|	|Mean dev|
Origi nal	-0,0 64	-0,0 94	3, 28	-3,2 8	-3,38	2,34
D1	0	0	0, 33	-3,3	0,19	0,19

Nor mal	me d	ma ks	mi n	Std ev	|Med dev|	|Mean dev|
D2	0	0	0,59	-0,59	0,36	0,38
D3	0	0	1,1	-1,1	0,7	0,71

Table 5. Sef 10% Current Feature

Signal Feature						
Nor mal	**me d**	**ma ks**	**mi n**	**Std ev**	**|Med dev|**	**|Mean dev|**
Origi nal	-0,0 64	-0,0 94	5,37	-5,37	-5,37	5,37
D1	0	0	0,38	-0,38	0,21	0,21
D2	0	0	0,62	-0,62	0,23	0,23
D3	0	0	1,2	-1,2	0,8	0,8

Table 6. Sef 24% Current Feature

Signal Feature						
Nor mal	**me d**	**ma ks**	**mi n**	**Std ev**	**|Med dev|**	**|Mean dev|**
Origi nal	-0,0 64	-0,0 94	9,2 68	-9,2 68	-8,35	8,37
D1	0	0	1,3 6	-1,3 6	1,32	1,32
D2	0	0	1,8 3	-1,8 3	0,56	0,56
D3	0	0	1,6 4	-1,6 4	0,81	0,81

Table 7. Inner Race Fault Current Feature

Signal Feature						
Nor mal	**me d**	**ma ks**	**min**	**Std ev**	**|Med dev|**	**|Mean dev|**
Orig inal	-0,0 64	-0,0 94	10, 381	-10, 381	-10,23 2	10,23 2
D1	0	0	1,4 5	-1,4 5	0,19	0,19
D2	0	0	1,9 3	-1,9 3	0,36	0,36

Nor mal	me d	ma ks	min	Std ev	|Med dev|	|Mean dev|
D3	0	0	1,7 2	-1,7 2	0,7	0,7

Table 8. Outer Race Fault Current Feature

Signal Feature						
Nor mal	**me d**	**ma ks**	**min**	**Std ev**	**|Med dev|**	**|Mean dev|**
Orig inal	-0,0 64	-0,0 94	11, 128	-11, 128	-11,12 1	11,12 1
D1	0	0	1,5 1	-1,5 1	1,32	1,32
D2	0	0	2,1	-2,1	1,21	1,21
D3	0	0	1,7 4	-1,7 4	1,1	1,1

Table 9. Rolling Element Current Feature

Signal Feature						
Nor mal	**me d**	**ma ks**	**min**	**Std ev**	**|Med dev|**	**|Mean dev|**
Orig inal	-0,0 64	-0,0 94	11, 218	-11, 218	-11,32 1	11,32 1
D1	0	0	1,7 4	-1,7 4	1,321	1,321
D2	0	0	2,4 5	-2,4 5	1,28	1,28
D3	0	0	1,8 34	-1,8 34	1,324	1,324

4.2 Evaluation of System Performance

Tests carried out on data that has been given accuracy of a uniform percent, in other words all tests of the state of the motor can be recognized properly. The test results can be displayed in a table as can be seen in table 10.

Table 10. Output Value Of Each Neuron

Condition of Induction Motor	Output NN			
	Neuron 1	Neuron 2	Neuron 3	Neuron 4
Normal	0.9949	0.0056	0.0019	0.0014
SEF 10%	0.0052	0.9945	0.0017	0.0015
SEF 24%	0.0017	0.0020	0.9975	0.0023
Inner Race Fault	0.0002	0.0027	0.0025	0.9979

Outer Race Fault	0.0006	0.0024	0.0045	0.9993
Rolling Element	0.0009	0.0036	0.0049	0.9987

Outer Race Fault	0%	0%	0%	0%	0%	100%
Rolling Element	0%	0%	0%	0%	0%	100%

After learning about the six features of the current signal feature, testing is done with data that has never been taught before. The main objective is to determine the validation of the paramaeter that has been used. The output of NN on testing valid data can be seen in table 11.

Table 11. Output NN

No.	Neuron 1	Neuron 2	Neuron 3	Neuron 4
1	**0.994865**	0.005531	0.001798	0.001275
2	**0.801184**	0.129708	0.001028	0.001214
3	**0.994865**	0.005532	0.001798	0.001279
4	**0.800332**	0.135144	0.001144	0.001193
5	**0.829851**	0.173738	**0.870067**	0.000435
6	0.008018	**0.996122**	0.001658	0.001584
7	**0.708085**	0.080635	0.010128	0.003154
8	0.014521	**0.963162**	0.001243	0.001383
9	**0.828596**	0.315685	0.000497	0.000668
10	0.072368	**0.718822**	0.000065	0.002365
11	0.001648	0.001942	**0.997443**	0.002238
12	0.004138	0.001215	**0.996643**	0.001511
13	0.001648	0.001942	**0.997443**	0.002238
14	0.004196	0.000992	**0.996544**	0.001972
15	0.004192	0.000992	**0.996543**	0.001972
16	0.000078	0.002644	0.002442	**0.997771**
17	0.000078	0.002644	0.002442	**0.997771**
18	0.000078	0.002644	0.002445	**0.997771**
19	0.000121	0.016348	0.005541	**0.996752**
20	0.000324	0.006803	0.000975	**0.995167**

Based on table 11, the NN identification results can be grouped based on the condition of induction motor bearing damage. NN identification results based on bearing damage conditions can be seen in table 12.

Table 12. Output Identification

Condition of Induction Motor	Output NN					
	Normal	SEF 10%	SEF 24%	Inner Race Fault	Outer Race Fault	Rolling Element
Normal	80%	0%	0%	0%	0%	0%
SEF 10%	43%	60%	0%	0%	0%	0%
SEF 24%	0%	0%	0%	98%	0%	0%
Inner Race Fault	0%	0%	0%	0%	0%	87%

5. CONCLUSION

Based on the analysis that has been done, the following conclusions can be drawn. The frequency domain signal from Matlab processing can represent the analyzed waveform so that it can be used as NN input. Training data was identified 100% and validation data identified an average of 86% in determining the state of three-phase induction motor bearings. The combination of the Fast Fourier transform used for continuous signal analysis and the NN method can be used to analyze and identify the type of interference.

6. DEVELOPMENT

This system can only be used to detect damage to induction motor bearings in a no-load condition, in the future it can be developed to detect motor winding damage with various kinds of expenses and damage that occurs.

REFERENCES:

[1] IEEE recommended practice for the design of reliable industrial and commercial power systems," IEEE Std. 2016 [IEEE Gold Book], Appendix H.

[2] Da Silva, A. M., *Induction Motor Fault Diagnostic and Monitoring Method,* Marquette University, Milwaukee, Mei 2006.

[3] Youb, Lamia. Effects of Unbalanced Voltage on the Steady State of the Induction Motors. International Journal of Electrical Energy, Vol. 2, No. 1, March 2014.

[4] Jover, P, Current, Force and Vibration-Based Techniques for Induction Condition Monitoring, TKK Dissertation 85, Helsinki University of technology, 2007.

[5] Mauridhi Hery P. dan Agus Kurniawan, "Supervised Neural Networks dan Aplikasinya", Graha Ilmu. Yogyakarta. 2006.

[6] Mauridhi Hery P. and Agus Kurniawan, "Supervised Neural Networks and Aplication", Graha Ilmu, Yogyakarta, 2006